

Enhanced Waters 2D Muscle Model for Facial Expression Generation

Dinesh Kumar and Dharmendra Sharma

Faculty of Science and Technology, University of Canberra, ACT, Australia

Keywords: Physics-based Model, Muscle Model, Facial Expression, Facial Animation, FACS.

Abstract: In this paper we present an improved Waters facial model used as an avatar for work published in (Kumar and Vanualailai, 2016), which described a Facial Animation System driven by the Facial Action Coding System (FACS) in a low-bandwidth video streaming setting. FACS defines 32 single Action Units (AUs) which are generated by an underlying muscle action that interact in different ways to create facial expressions. Because FACS AU describes atomic facial distortions using facial muscles, a face model that can allow AU mappings to be applied directly on the respective muscles is desirable. Hence for this task we choose the Waters anatomy-based face model due to its simplicity and implementation of pseudo muscles. However Waters face model is limited in its ability to create realistic expressions mainly the lack of a function to represent sheet muscles, unrealistic jaw rotation function and improper implementation of sphincter muscles. Therefore in this work we provide enhancements to the Waters facial model by improving its UI, adding sheet muscles, providing an alternative implementation to the jaw rotation function, presenting a new sphincter muscle model that can be used around the eyes and changes to operation of the sphincter muscle used around the mouth.

1 INTRODUCTION

A widely accepted theoretical foundation for the control of facial expression generation is the Facial Action Coding System (FACS). FACS is based on an anatomical analysis of facial movements and has been developed by psychologists P. Ekman and W.E Frieson (Ekman and Frieson, 1977). In 2002, a new version of FACS was published, with large contributions by Joseph Hager (Hager et al., 2002). It was designed primarily to measure facial movement relevant to emotion. The aim was to develop a comprehensive system which could distinguish all possible identifiable facial movements. Since every facial movement is the result of muscular actions on the face, to render FACS on a computer face model requires a model on which the FACS Action Units (AUs) can be easily mapped onto.

In this paper we present an improved Waters facial model used as an avatar for work published in (Kumar and Vanualailai, 2016), which describes a Facial Animation System (FAS) driven by FACS in a low-bandwidth video streaming setting. The overall aim is to prepare a facial model on which FACS AU activations can be directly applied onto

their corresponding facial muscle to generate an expression or combination of expressions. We note that the domain of computer facial modelling has advanced tremendously over the last decade as described by (Alkawaz et al., 2015) and focus has shifted more to non-muscle based systems. However work dedicated to enhancement of muscle based models in recent years has been few and limited. Our reasons for selection of Water muscle model have been due to its simplicity, implementation of pseudo muscles and the availability of the software in C++ for the basic model. However Waters face model comes with limitations in its ability to create realistic expressions; mainly the lack of a function to represent sheet muscles, unrealistic jaw rotation function and improper implementation of sphincter muscles. Hence in this paper we present a thorough investigation of the Waters muscle-based model and provide enhancement to the basic model by:

- adding sheet muscles;
- providing an alternate implementation to the jaw rotation function;
- presenting a new sphincter muscle equation that can be used around the eyes;
- changes to operation of the sphincter muscle used around the mouth; and

- improving its UI

Through this work we would also like to highlight the importance of developing muscle-based models to represent the anatomy of the human face more accurately in order to generate realistic expressions. The rest of the paper is organised as follows: In section 2 we review related work in the field of facial modelling. Section 3 describes our *Facial Model* component FAS. In section 4, we present the implementation and test results followed by conclusion in section 5.

2 RELATED WORK

Initial efforts in 3D facial modelling began with (Parke, 1972) who developed the first parameterized facial model. (Waters, 1987) and (Magenat-Thalmann et al., 1988) follow soon by developing pseudo muscle based models. The technique of free form deformations were also used to create facial expressions for example in (Kalra, et al., 1992). (Kahler et al., 2001) utilised geometry based muscle modelling for facial animation whereas (Ostermann, 1998) used the MPEG-4 standard to animate synthetic faces.

The state of the art in facial animation has advanced tremendously over the years. There is increasing effort by researchers to perfect the facial model to produce quality and realistic expressions. As a consequence some new and hybrid methods are continuously being developed using FACS (Tolba et al., 2018). For example an interactive region-based linear 3D face model, developed by (Tena et al., 2011) effectively divided the facial model into regions with user-given constraints in the form of markers placed on the face model. These markers when activated affected only the region in which they were placed and produced better effects than using the same markers on a region less model. (Lewis et al., 2014) in their paper discuss the practice and theory of blend shape models. Real time performance based facial animation that enables the user to control the facial expression of a digital avatar in real-time is proposed by (Weise et al., 2011). (Pauly, 2013) and (Bermano et al., 2013) proposed similar facial performance based models. There has also been success in producing facial animation from video or motion capture data. A paper by (Sifakis et al., 2005) described an implementation where muscle activations were automatically determined from motion capture marker data. Motion detectors or sensors that are susceptible to movements can be utilised to detect

facial expressions and then animated on a computer facial model.

Recent research has shown a renewed interest in using FACS as the basis for generating and measuring facial expressions. For example (Alkawaz et al., 2015) combined blend shape interpolation (BSI) and FACS to create realistic and expressive facial animation. They trialled their system on four basic emotions; anger, happy, sad, and fear defined in FACS. (Tolba et al., 2018) discussed the applications and limitations of FACS by comparing with MPEG-4 facial animation based systems. Articles such as (Ping et al., 2013; Li et al., 2012; Sandbach et al., 2012; Ersotelos and Dong, 2008; Alkawaz et al., 2014) provide a good survey of techniques developed in the area of facial modelling in recent times while (Noh and Neumann, 1998) provides a review on theories and techniques developed decades ago which are a foundation of facial modelling techniques of the modern world.

3 FACIAL MODEL IN FAS

In this research we use the Facial Animation System (FAS) described in (Kumar and Vanualailai, 2016). The original Waters face geometry is retained and used in the *Facial Model* component in FAS. It is based on facial anatomy which dictates that facial expressions are created by relaxation and tightening of facial muscles. These muscles on the face can be categorized into three types: linear muscles, sheet muscles and sphincter muscles. Mixtures of these muscle types coordinate to produce each facial expression.

Waters modelled two types of muscles: linear muscles that pull vertices under its region of influence towards the point of attachment on the skin; and a sphincter muscle around the mouth that pulls the vertices under its region of influence towards the center of an ellipse. The third muscle type (sheet muscles) was not implemented in the original Waters model but was described in detail in (Zhang et al., 2001). The equations we use in this paper are drawn from (Tanguy, 2001; Edge and Maddock, 2001) which is based on the original Waters model publication, but expressed in a simplified form for understanding. The geometry comprises of 236 interconnected vertices forming 876 triangular polygons. The reader is directed to (Waters, 1987) to inspect the original visual representation of the muscles and the facial model.

In our *Facial Model* we reduced the number of linear muscles from 24 to 18. Figure shows the

linear muscles retained in our model. Comparing this with Waters model one can note that linear muscles around the mouth have been removed as they produced unrealistic expressions on the facial model. They have been replaced a sphincter muscle. We omit the discussion of the equations of the linear muscle in this paper as this is about the only change that was made to this vector muscle. The reader is directed to (Waters, 1987) for a full description of linear muscles.

3.1 Enhancements to Waters Model

In the following sub sections we describe the equations of the sphincter and sheet muscles and modifications to the original model equations to bring about enhancements to the Waters face model to a level that allowed us to use it in FAS. We also describe the new jaw rotation function and improvements in the user interface to enable recordings of expressions defined by AUs.

3.1.1 Sphincter Muscles

The sphincter muscle is modeled by Waters as an elliptical shape and can be simplified to a parametric ellipsoid. Vertices within the ellipsoid are drawn towards the center of the ellipsoid (like a drawstring bag) with maximum movement depended on how far the vertex position is from the center of the ellipsoid. Figure 1 and Figure 2 illustrate the sphincter muscle in the x, y plane with the following definitions:

- P : An arbitrary facial skin point.
- c : Epicenter of the sphincter muscle influence area.
- lx : The semi-major axis of the sphincter muscle influence area.
- ly : The semi-minor axis of the sphincter muscle influence area.

The following equation therefore can be used to compute the new position p' of the vertices at an arbitrary point P in the x, y plane within the ellipsoid.

$$p' = P + KD \frac{\overrightarrow{Pc}}{|\overrightarrow{Pc}|} \quad (1)$$

where K is the muscle spring constant and D is calculated as:

$$D = \begin{cases} fg & \text{for } |\overrightarrow{Pc}| > ly \\ 0 & \text{for } |\overrightarrow{Pc}| \leq ly \end{cases} \quad (2)$$

where f is the coefficient of the vertex displacement for the sphincter muscle in the $x - y$ plane, and g is the proportional distance of the vertex position from the center of the ellipse, i.e.,

$$f = 1 - \frac{\sqrt{ly^2 P_x^2 + lx^2 P_y^2}}{lxly} \quad (3)$$

$$g = \frac{|\overrightarrow{Pc}|}{lx} \quad (4)$$

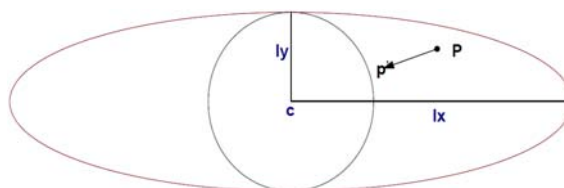


Figure 1: Sphincter muscle model.

The calculation of D above protects the central area of the ellipse (bounded by a circle with radius equal to ly) from vertices from piling up on top of each other towards the center of the ellipse by muscle contractions.

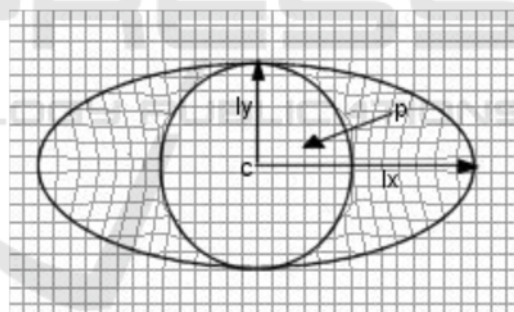


Figure 2: Vertices contracting towards center of sphincter muscle. (Edge and Maddock, 2001).

Equations 1-4 simulate the working of the sphincter model in 2D. In real lips, the skin protrudes (bulges) towards the center of the lips, hence displacement in the z axis is needed for 3D visualisation. This can be achieved by calculating for p'_z as:

$$p'_z = P_z + \frac{K(1-fg)}{Z} \quad (5)$$

where Z is a constant greater than 0 and is used to control the peak of the protrusion. Implementation of the sphincter muscles around the mouth is shown in Figure 3. The example expression is created with

$K = 0.3$ and $Z = 10$. In this paper we modify the original Waters program to use three sphincter muscles; one each around the eyes and one covering the mouth opening area. The sphincter muscle used around the mouth area is derived from Waters original sphincter muscle equation where the vertices converge towards the centre of the muscle. However the orbicularis oris muscle that surrounds the eye behaves a bit differently. It does not have the ability to pull the corners of the eyelids towards the center of the eye. Instead it is only able to pull the upper and lower eyelids towards each other. Hence to use the above sphincter equations for the eyes it had to be modified so that the vertices converge towards the semi-major axis of the ellipse defining the influence area around the eyes. This gives the model the ability to “squint” eyes.



Figure 3: Application of the sphincter muscle on the area around the mouth.

Figure 4 illustrates our eye sphincter muscle in the xy plane with the same definitions as for the normal sphincter muscle. We note here that the displacement is along the x -axis. The new equation to compute the new position p' of the vertices at an arbitrary point P in the xy plane within the ellipsoid in Figure 5 is:

$$p' = P + KD \frac{\overline{Px}}{|Px|} \quad (6)$$

where K is the muscle spring constant and is calculated as:

$$D = fg \quad (7)$$

Here, f is the coefficient of the vertex displacement for the sphincter muscle along the y -axis plane and g is the proportional distance of the vertex position perpendicular to the x -axis, i.e.,

$$f = 1 - \frac{\sqrt{ly^2 P_y^2}}{ly} \quad (8)$$

$$g = \frac{|\overline{Px}|}{ly} \quad (9)$$

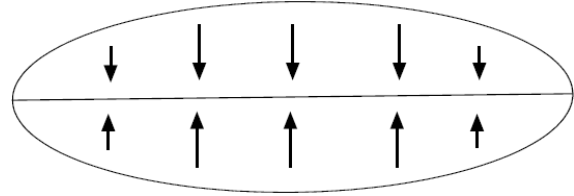


Figure 4: Vertices converging to the semi-major axis.

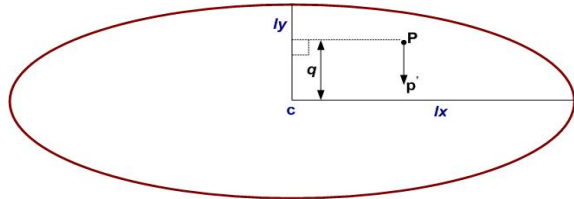


Figure 5: Sphincter muscle diagram for use around the eyes.



Figure 6: Using sphincter muscles around the eyes. $K = 0.2$ for left eye (to the reader) and $K = 0.4$ for the right eye. $Z = 30$.

For displacement in the x -axis direction, the same formula as equation (5) is re-used, where Z is a constant greater than 0. A small value for Z causes the eyelids to bulge out, hence in our implementation we have set this constant to 30, which achieves good results. Figure 6 shows a visual of the application of the new sphincter muscle activation around the left eye.

3.1.2 Sheet Muscle Model

Unlike the linear and sphincter muscle, sheet muscles are made up of a series of almost-parallel fibres spread over a rectangular area. The displacement of vertices therefore is towards one end of the rectangle with the other end of the

rectangle attached to the bone with maximum displacement towards the attachment point of the sheet muscle to the bone. In anatomy, sheet muscles models muscles such as the frontalis which is located on the forehead on a human face. Waters in his face program instead used linear muscles for the forehead and do not provide a description of sheet muscles in (Waters, 1987). Hence we use the description of sheet muscles from (Zhang et al., 2001). However to achieve the desired effect in our effort to produce realism in the expressions created we use Waters linear muscles combined with two sheet muscles (one on each side of the forehead).

Figure 7 illustrates the sheet muscle with the following definitions:

- P : An arbitrary facial skin point.
- A_1, A_2 : Boundary points defining the attachment line of sheet muscle to bone.
- l_1, l_2 : Boundary points defining the insertion line of sheet muscle to skin.
- A_c : Middle point of sheet muscle attachment line.
- l_c : Middle point of sheet muscle insertion line.
- L, W : Length and width of the rectangle defining the zone of influence of the sheet muscle respectively.
- l_i : Distance between arbitrary skin point P and the attachment line.

The new position p' of the vertices at an arbitrary point P in the x, y, z plane within the rectangular zone of influence can be calculated as.

$$p' = KD \frac{\overline{A_c l_c}}{\left| \overline{A_c l_c} \right|} \quad (10)$$

where i indicates the values of the x, y, z coordinates of the vertex. Here, K is the muscle spring constant and D is calculated as:

$$D = \begin{cases} \cos\left(\frac{(1-\lambda^n)\pi}{2}\right) & \text{for } 0 \leq \lambda \leq 1 \\ \cos\left(\frac{(\lambda^n-1)\pi}{2}\right) & \text{for } 1 < \lambda \leq \delta \end{cases} \quad (11)$$

where n is the sheet muscle strength factor and set at 1 in our implementation. Here, λ_i and δ are calculated as:

$$\lambda_i = \frac{q}{\left| \overline{A_c l_c} \right|} \quad (12)$$

$$\delta = \frac{L}{\left| \overline{A_c l_c} \right|} \quad (13)$$

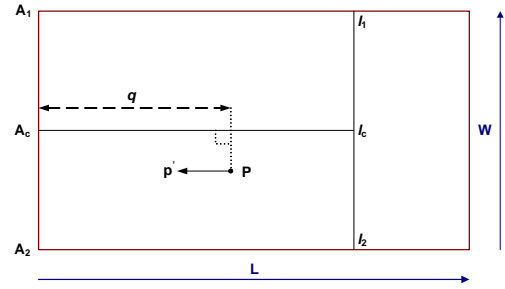


Figure 7: Sheet muscle model.

The relationship between the rectangular sheet muscle and the arbitrary point P is shown in Fig. Therefore q can be calculated using the following:

$$q = \left| \overline{AP} \right| \cos \Omega \quad (14)$$

$$\text{where } \Omega = \arccos \left(\frac{\overline{AP} \cdot \overline{AB}}{\left| \overline{AP} \right| \left| \overline{AB} \right|} \right) 180 / \pi \quad (15)$$

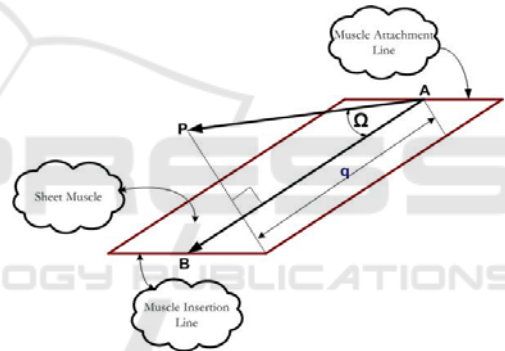


Figure 8: Relationship between P and the sheet muscle for calculation of q .

The placement of sheet muscles on our face geometry and its effect on raising the forehead is shown in Figure 9.

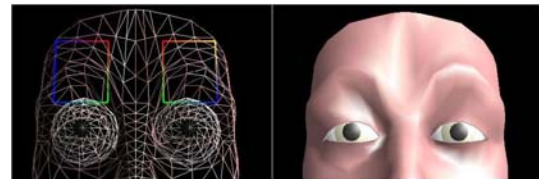


Figure 9: Implementation of the sheet muscles. $K = 0.4$, $L - \left| \overline{A_1 l_1} \right| = 2$.

3.1.3 Jaw Rotation

In order to create more convincing expressions it is important for the facial model to allow for jaw

rotations. The human jaw is made up of two parts namely the upper and lower jaw. The upper jaw remains fixed while it is the lower jaw that moves. Waters models the moving lower jaw relative to the pivot point of the facial model mesh rather than employing any muscle technique. In his model the jaw contains vertices of the lower part of the face which is rotated along the y -axis and z -axis. Hence this rotation can be explained using the following definitions and equations.

P : Vertex forming the lower jaw.

K : Angle of rotation of the jaw vertex relation to the root of the facial mesh and is a value between 0 and 4 with 4 indicating the maximum opening.

$$p'_y = \cos\left(\frac{K\pi}{180}\right)P_y + \sin\left(\frac{K\pi}{180}\right)P_z \quad (16)$$

: for rotation along y -axis

$$p'_z = \sin\left(\frac{K\pi}{180}\right)P_y + \cos\left(\frac{K\pi}{180}\right)P_z \quad (17)$$

: for rotation along z -axis

This formula is applied on all vertices that form the jaw. The animator therefore has to specify manually in advance which vertices would be part of the jaw of the face. Adjusting the value of K simulates jaw opening and closing with maximum rotation produced at the center of the lower lip. This however creates discontinuity at the corners of the lips as reported by (Zhang et al., 2001) and illustrated Figure 10. To keep the cohesion at the corner of the lips we have given each vertex forming the moveable part of the lower jaw a weight value in the range 0.0 to 1.0 depending on its proximity to the center of the lips. Since the formula above created maximum rotation at the center of the lip, all vertices of the lower jaw around the center are allocated a higher weight value with decreasing weights towards the corner of the lips. Hence the corner points of the lips are allocated a weight of 0 meaning no rotation.



Figure 10: Discontinuity at the lip corners. (Parke and Waters, 1996).

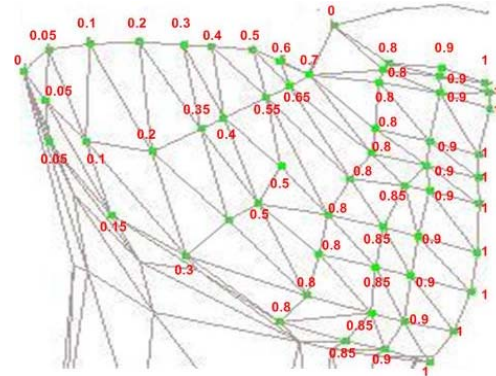


Figure 11: Weights allocated to vertices forming the lower part of the jaw.



Figure 12: Jaw drop correction.

Figure 11 illustrates the allocation of weights to vertices forming the lower jaw. After p' has been determined from equations (16) and (17), it is fed into the following two equations to determine the final position of vertex P . Here w is the weight at P . Figure 12 shows the improvement in the jaw rotation function.

$$p''_y = p'_y w + P_y (1 - w) \quad (18)$$

: for rotation along y -axis

$$p''_z = p'_z w + P_z (1 - w) \quad (19)$$

: for rotation along z -axis

4 IMPLEMENTATION IN FAS

The original Waters face geometry is retained and used in our project. In addition to the 18 linear muscles, our model introduces 2 sheet muscles and 3 sphincter muscles. Figure 13 shows all the implemented muscles in our model. The manipulation of these muscles to generate facial expressions is handled via the *Expression Editor* in FAS (Kumar and Vanualailai, 2016). Given the nature of this research the realism of the expression generated is validated by visual inspection using FACS as a guide.

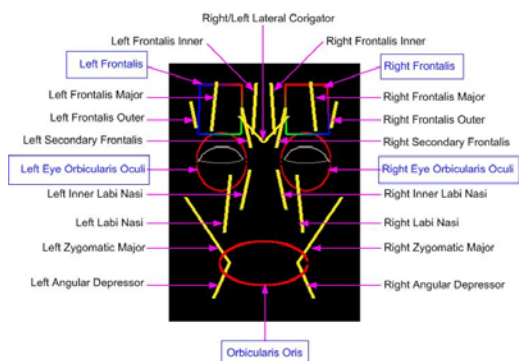


Figure 13: Implemented muscles in our *Facial Model*.

4.1 Expression Editor

The *Expression Editor* in FAS gives the user control over all the muscles (including the jaw) used in our face model hence allowing a wide range of expressions to be generated with ease. Since our aim is to animate facial expression based on FACS AUs, it gives the flexibility to generate expressions that can approximate the various AUs defined in FACS. Using the expression editor the user can manipulate one or more muscles to match a particular AU expression. During this activity the calibration is rendered in the graphics window for the user to note the deformations on the face model. This allows the user to fine tune the expression. Once the desired expression is generated to a satisfactory level it can then be recorded with the AU number as an identifier. There is also the possibility to modify an existing AU expression if desired by the user. A total of 64 AU expressions can be defined.

A minimum value of 0.0 and maximum value of 2.0 can be chosen as activation values for each muscle. Beyond activation value of 2.0 gives unrealistic results as far as facial mesh deformation is concerned. However the user can use a value from 0.0 to 4.0 (inclusive) for the jaw control.

By the definition of FACS, complex facial expressions are generated by applying one or more individual AUs. When these AU expressions are programmed and stored in our system, it gives us the possibility to generate many other compound expressions simply by using combinations of AUs.

4.2 Suitability of Waters Muscle Model for Facial Animation

Unlike techniques where producing animation requires direct manipulation of the facial mesh, Waters muscles are independent of the facial mesh. This means that the animator has the freedom to

change the facial mesh yet still achieve the same effect as in using the original mesh. This allows flexibility in using different character mesh topologies. It allows for compact representation of facial geometry where the only information needed are the muscle parameter values and the skin mesh data in order to produce expressions. The muscle functions work on triangulated vertices, which most graphics hardware are optimized to use, hence rendering is fast. Further expression parameters can control groups of muscles at once resulting in multiple muscle deformation applied to the facial mesh. The problem areas include the difficulty of placing muscles on the geometry of the face which obviously has to be done manually. The muscle functions basically represent flat architectures hence they may not be attached to the skin (facial mesh) at all. Due to this, muscle curvature and volume is also not taken into account. At times during animation some mesh vertices can fall prey to influence from multiple muscle actions, though this problem can be solved by taking “average” influences of the muscle on the vertex. Overall given that FACS AUs map directly to facial muscles, a muscle based model is desirable.

5 CONCLUSIONS

The Waters muscle model opens a gateway to excellent research in facial animation controlled by muscles. They have been used and tested widely by researchers over the years. Given the aim of our project to generate facial expressions governed by FACS, and that FACS basically describes expressions based on affected muscles on the face, Waters muscle model becomes the ideal choice for use since it allowed easy mapping with FACS AUs. However we do note the advancements in facial modelling techniques over the years which are not muscle based but may have potential in mapping with FACS AUs. The modular design of our FAS will allow our *Facial Model* component to be replaced with a different modeling technique with ease. Future directions of muscle based model will be the development of 3D muscles with different shape, size and volume to mimic natural muscles; expand and contract with volume displacement techniques. Using such design we shall be able to model real facial expression effects.

REFERENCES

- Alkawaz, M. H. et al. (2015). Blend Shape Interpolation and FACS for Realistic Avatar. *3D Research (Springer Link)*, 6(6).
- Alkawaz, M. H. et al. (2014). Facial Animations: Future Research Directions and Challenges. *3D Research (Springer Link)*, 5(12).
- Bermano, A. et al. (2013). Facial Performance Enhancement Using Dynamic Shape Space Analysis. *ACM Transactions On Graphics (ACM TOG)*.
- Edge, J. D. and Maddock, S. (2001). Expressive Visual Speech using Geometric Muscle Functions. *Proc. Eurographics UK*, pp. 11-18.
- Ekman, P. and Frieson, W. (1977). Facial action coding system. *Consulting Psychologists Press*.
- Ersotelos, N. and Dong, F. (2008). Building Highly Realistic Facial Animation: A Survey. *The Visual Computer*, 24(1), pp. 13-30.
- Hagar, J. C. et al. (2002). *Facial Action Coding System investigator's guide*, Salt Lake City, UT: A Human Face.
- Kahler, K. et al. (2001). Geometry-based muscle modeling for facial animation.. *In Proc. of Graphics Interface*, p. 37-46.
- Kalra, P. et al. (1992). Simulation of facial muscle actions based on rational free form deformations.. *In Proc. of Eurographics*, pp. 59-69.
- Kumar, D. and Vanualilailai, J. (2016). Low Bandwidth Video Streaming using FACS, Facial Expression and Animation Techniques. *Proceedings of the 11th Joint Conference on Computer Vision, Imaging and Computer Graphics Theory and Applications (VISIGRAPP 2016)*, Volume 1, pp. 226-235.
- Lewis, J. P. et al. (2014). Practice and Theory of Blendshape Facial Models. *EUROGRAPHICS State of the Art Reports 2014*.
- Li, L. et al. (2012). A Survey of Computer Facial Animation Techniques. *International Conference on Computer Science and Electronics Engineering*.
- Magenat-Thalmann, N. et al. (1988). Abstract muscle action procedures for human face animation. *Visual Computer*, 3(5), pp. 290-297.
- Noh, J. and Neumann, U. (1998). A Survey of facial Modeling and Animation Techniques. *Technical Report, University of Southern California*.
- Ostermann, J. (1998). Animation of synthetic faces in MPEG-4. *Computer Animation*, pp. 49-51.
- Parke, F. (1972). Computer generated animation of faces. *ACM Annual Conference*.
- Parke, F. and Waters, K. (1996). *Computer Facial Animation*. s.l.:A K Perters Wellesly.
- Pauly, M. (2013). Realtime Performance-Based Facial Avatars for Immersive Gameplay. *Proceedings of the ACM SIGGRAPH Conference on Motion in Games 2013*.
- Ping, H. et al. (2013). Computer Facial Animation: A Review. *International Journal of Computer Theory and Engineering*, 5(4).
- Sandbach, G. et al. (2012). Static and Dynamic 3D Facial Expression Recognition: A Comprehensive Survey. *Image Vision Computing*, 30(10), pp. 683-697.
- Sifakis, E. et al. (2005). Automatic determination of facial muscle activations from sparse motion capture marker data. *ACM. Trans. on Graphics (SIGGRAPH)*.
- Tanguy, E. (2001). An Abstract Muscle Model for Three Dimensional Facial Animation. *Technical Report, University of Sheffield, UK*.
- Tena, J. R. et al. (2011). Interactive Region-Based Linear 3D Face Models. *SIGGRAPH*.
- Tolba, R. M. et al. (2018). Realistic Facial Animation Review: Based on Facial Action Coding System. *Egyptian Computer Science Journal*, 42(1).
- Waters, K. (1987). A Muscle Model for animating 3D facial expressions. *Computer Graphics (SIGGRAPH'87)*, 21(4), pp. 17-24.
- Weise, T. et al. (2011). Realtime Performance-Based Facial Animation. *Transactions on Graphics (Proceedings SIGGRAPH 2011)*, 30(4).
- Zhang, Y. et al. (2001). Animation of Facial Expressions by Physical Modelling. *EuroGraphics*.